NÖHÜ Müh. Bilim. Derg. / NOHU J. Eng. Sci., 2022; 11(3), 776-780

Niğde Ömer Halisdemir Üniversitesi Mühendislik Bilimleri Dergisi
Niğde Ömer Halisdemir University Journal of Engineering Sciences

Araştırma makalesi / Research article

www.dergipark.org.tr/tr/pub/ngumuh / www.dergipark.org.tr/en/pub/ngumuh

Preparation of high solid loading and low viscosity ceramic slurry for dip-coating method

Daldırarak kaplama yöntemi için katı yüklemesi yüksek ve viskozitesi düşük seramik kaplama çözeltisinin hazırlanması

Berceste Beyribey[1,*], Joshua Persky[2]

[1,2] *Low Emissions Resources Global Ltd., Unit 2 Block A, Mid Craigie Industrial Estate, Mid Craigie Road, Dundee UK, DD4 7RH*

Abstract

$BaCe_{0.7}Zr_{0.1}Y_{0.16}Zn_{0.04}O_{3-\delta}$ (BCZYZ) ceramic slurry has been prepared with different solid loading and the maximum solid loading of the slurry has been predicted as 25 vol.% using the Krieger-Dougherty equation. The slurry with the maximum solid loading has been formulated and applied as an electrolyte on porous NiO/BCZYZ tubular supports by the dip-coating method. Cells sintered at 1500°C for 10h have been characterised by Scanning Electron Microscopy (SEM) analysis. The 30µ thick, very dense electrolyte layer has successfully been achieved with some closed pores.

Keywords: Ceramic electrolyte, Dip-coating, NiO/BCZYZ, SOFC

Öz

Farklı katı yüklemelerine sahip $BaCe_{0.7}Zr_{0.1}Y_{0.16}Zn_{0.04}O_{3-\delta}$ (BCZYZ) seramik çözeltileri hazırlandı ve çözelti için maksimum katı yüklemesi Krieger- Dougherty eşitliği yardımı ile hacimce %25 olarak belirlendi. Maksimum katı yüklemesine sahip kaplama çözeltisi hazırlanarak, daldırarak kaplama yöntemi ile elektrolit olarak gözenekli NiO/BCZYZ tüp seklindeki desteklerin üzerine kaplandı. 1500°C'deki 10 saatlik sinterleme işleminden sonra, taramalı elektron mikroskopu yardımı ile elektrolit karakterize edildi. 30µ kalınlıkta, kapalı gözenekler içeren, geçirimsiz elektrolit kaplaması elde edildi.

Anahtar kelimeler: Seramik elektrolit, Daldırarak kaplama, NiO/BCZYZ, KOYP

1 Introduction

Solid oxide fuel cells (SOFCs) and solid oxide electrolysers (SOECs) are very efficient energy conversion devices, which are normally operated at high temperatures in the range of 600 - 1000 ˚C. Ni-YSZ based supports are mainly used in SOFCs and SOECs owing to its high conductivity, electrochemical activity, and low electrode polarization [1-3]. Recently, the research has been focused on Ni-BCZY based supports. Proton conducting materials are advantageous over oxygen ion conducting one due to the reduced operating temperatures preserving the high conductivity and chemical stability [4-6]. Planar and tubular SOFCs and SOECs are conventionally used for different applications. While the planar cells are attractive for stationary application due to their long start up time, the tubular cells are more beneficial for mobile application due to their short start-up time [7]. The other advantageous of tubular SOFCs and SOECs are mechanical strength, high volumetric power density, high thermal cyclic behaviour and less problematic sealing compared to the planar ones [8,9].

One of the main components of SOFCs and SOECs is the ceramic electrolyte, and it is critical to have a dense and open porosity free electrolyte to achieve high efficiencies. The quality of the electrolyte is strongly dependent to the fabrication methods and dip-coating is one of the most widely used coating technique in the ceramic industry due to being a simple, cost effective and time effective method [10-12]. It can easily be applied on substrates in various geometric shapes and has a great potential to be used for large-scale commercial production [10,11,13]. Slurry characteristics such as viscosity and solid loading of the slurry strongly affects the dip coating quality and subsequent electrolyte performance [14]. While the low viscosity is important to obtain a thinner and satisfactory electrolyte coating, high solid loading is crucial to achieve a dense and crack-free electrolyte [15]. Therefore, it is essential to achieve high solid loading and low viscosity ceramic slurries to achieve high quality electrolyte coating. There are various semi-empirical models to predict the maximum solid loading of ceramic slurries and Krieger-Dougherty model is one of the widely used one in the literature [16-20].

In this work, the maximum solid loading has been predicted for BCZYZ slurry using Krieger-Dougherty model, and BCZYZ slurry with maximum solid loading has been prepared and applied as electrolyte on tubular NiO/BCZYZ supports by dip-coating technique.

2 Material and methods

$BaCe_{0.7}Zr_{0.1}Y_{0.16}Zn_{0.04}O_{3-\delta}$ (BCZYZ) was synthesized using combustion spray pyrolysis (Praxair Specialty Ceramics). The powder was dried at 95°C for 24 h to minimize water content before sieving through 320 mesh. The coating slurry was prepared by mixing BCZYZ powder and Butanol (Sigma, Aldrich) with a various solid loading in the range of 8-23 vol.% as given in the Table 1. The slurry was milled on a roller mill for 24 h in total.

* Sorumlu yazar / Corresponding author, e-posta / e-mail: b_berceste@hotmail.com (B. Beyribey)
Geliş / Recieved: 02.04.2022 Kabul / Accepted: 27.05.2022 Yayımlanma / Published: 18.07.2022
doi: 10.28948/ngmuh.1096585

Table 1. Solid loading of the samples

Sample Name	vol.% BCZYZ	wt.% BCZYZ
SL-08	8	40
SL-10	10	45
SL-12	12	50
SL-14	14	55
SL-16	16	60
SL-19	19	65
SL-23	23	70

The stability of the BCZYZ powder in butanol was studied as a function of solid loading through zeta potential measurement and sedimentation. The slurry samples were transferred to the 10 ml graduated cylinders and then allowed to settle for 12 days. The zeta potential measurements were done at the 1st day using a zeta potential analyser (Zetasizer Nano Z, Malvern, UK).

The rheological behaviour and apparent viscosity of the slurries were determined using a rheometer (Kinexus Pro+, Malvern, UK). The critical ceramic powder volume concentration was determined using Krieger-Dougherty Model and a dip coating slurry was prepared for the critical volume concentration, including polyvinylpyrrolidone (Sigma, Aldrich) and Butvar (Sigma, Aldrich) as binders and, Dibutyl phthalate (Sigma, Aldrich) and Polyethylene Glycol (Sigma, Aldrich) as plasticisers.

L025 NiO/BCZYZ tubular ceramic support (Low Emissions Resources Global Ltd., UK) was used as substrate in the experiments. The tubular support was pre-fired at 1200°C for 3h (Top Hat Furnace, Deltech, US) to achieve a porous structure before coating. A tubular support was coated using the slurry with the maximum solid loading. A built-in house instrument was used for dip-coating, applying 9.53 mm·sec-1 immersion speed, 3.0 mm·sec-1 withdrawal speed and 30 second dwell time. The coated cells were then placed in a built-in house drying cabinet set at 40°C for 1 hour before sintering at 1500°C for 10 hours.

The fully fired half-cell was cut using a diamond saw (Smart Cut 6001, UKAM Industrial Superhard Tools, CA, USA) to get samples from middle of cells for image analysis using Scanning Electron Microscope (SEM) (Hitachi TM4000Plus).

3 Results and discussions

Figure 1 presents the effect of solid loading on the rheological behaviour and the viscosity of BCZYZ slurry. In general, the difference in the rheological behaviour at different solid loading is negligible. The slurry shows shear-thinning behaviour at low shear rates and Newtonian behaviour at middle and high shear rates. While the Newtonian behaviour is seen above 2 s^{-1} shear rates up to 16 vol.% solid loading, it is shifted to the higher shear rates above that solid loading. While the apparent viscosity is ~0.2 Pa·s at the shear rate of 2 s^{-1} up to 16 vol.% solid loading, it increases to 2.3 Pa·s and 9.9 Pa·s by increasing the solid loading to 19 vol.% and 23 vol.%, respectively.

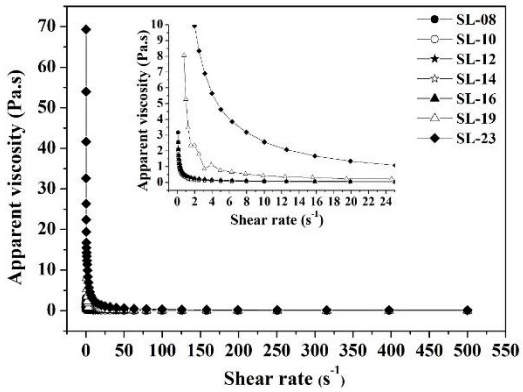

Figure 1. The effect of the solid loading on the rheological behaviour and viscosity

As seen in Figure 2, the change in the apparent viscosity at 20 s^{-1}, 100 s^{-1} and 200 s^{-1} shear rates versus solid loading fits well with an exponential model (R^2 = 0.999) and the difference in the apparent viscosity at different shear rates becomes significant above 16 vol.% solid loading. The model parameters are given in the Table 2.

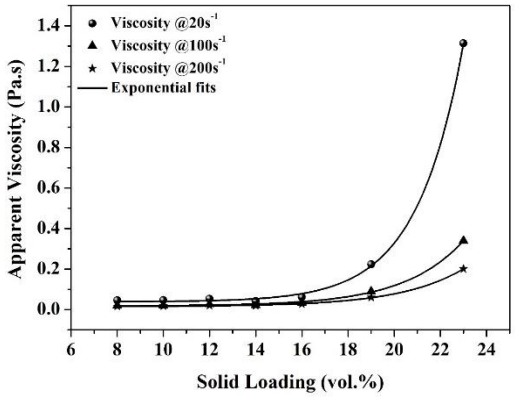

Figure 2. Apparent viscosity of the slurries versus solid loading

Table 2. Exponential model parameters

Exponential Model: $y = a + b * e^{cx}$	Model Parameters			
Shear rate	**a**	**b**	**c**	**R^2**
20 s^{-1}	0.039	1.47x10^{-5}	0.50	0.999
100 s^{-1}	0.018	4.41x10^{-5}	0.39	0.999
200 s^{-1}	0.015	4.38x10^{-5}	0.36	0.999

Figure 3 gives the correlation between zeta potential and solid loading. While the zeta potential is negative up to 10 vol.% solid loading, it becomes positive with 12 vol.% solid loading. From the graph, the isoelectric point is found out as 11 vol.% of BCZYZ. At the vol.% values above the isoelectric point, the negative surface species predominates, while at the vol.% values below the isoelectric point, the positive surface species predominates. Figure 4 indicates that the sedimentation rate is quite higher under the isoelectric point and becomes significantly stable at 16 vol.% solid loading and above.

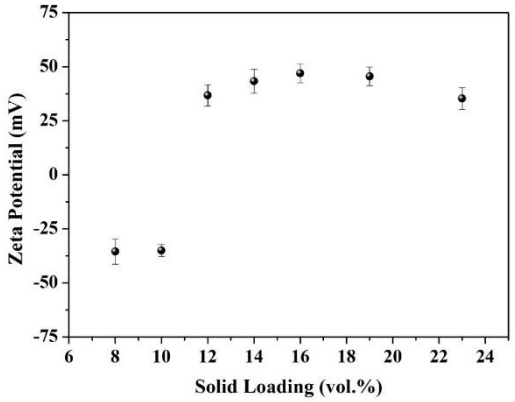

Figure 3. Zeta potential versus solid loading

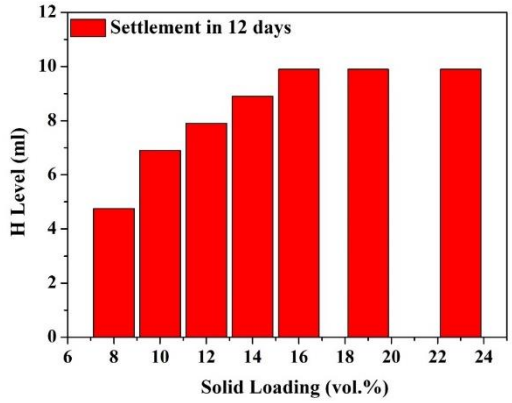

Figure 4. Sedimentation rate versus solid loading

Various semi-empirical models allow to predict the maximum solid loading for ceramic suspensions [17-20]. In the present work, the most widely used Krieger-Dougherty equation is considered [17]:

$$\eta = \eta_0[1 - (\emptyset/\emptyset_m)]^{-[\eta]\emptyset_m} \quad (1)$$

Where, η is the viscosity of the suspension, η_0 is the viscosity of the fluid phase of the suspension, $\emptyset$ is the fraction in volume of the disperse solid phase of the suspension, $\emptyset_m$ is the maximum solid loading, $[\eta]$ is the intrinsic viscosity. Equation (1) is linearized in Equation (2) to determine the best fit parameters using the apparent viscosity with various solid loadings:

$$\ln \eta = -[\eta]\emptyset_m \ln(1 - \emptyset/\emptyset_m) + \ln \eta_0 \quad (2)$$

The parameter $\emptyset_m$ is determined by choosing the value of $\emptyset_m$ to give the best fit straight line through the graph given in the Figure 5. By maximizing the R^2, $\emptyset_m$ is found as 0.25 at the high and medium shear rates and 0.24 at low shear rates. The model parameters are given in the Table 3.

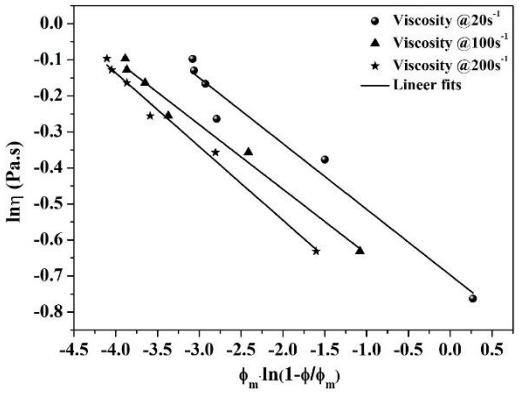

Figure 5. $\ln \eta$ plotted against $\emptyset_m \ln(1 - \emptyset/\emptyset_m)$

Table 3. Linear model parameters

Linear Model: $y = a + bx$	Model Parameters		
Shear rate	**a**	**b**	**R^2**
20 s^{-1}	-0.182	-0.697	0.961
100 s^{-1}	-0.179	-0.818	0.98
200 s^{-1}	-0.955	-0.205	0.987

The pre-fired porous L025 NiO/BCZYZ tubular ceramic support was coated with BCZYZ slurry with the maximum solid loading and analysed using SEM. Figure 6 presents the SEM images of the surface and fractured of the BCZYZ layer, which indicates a very dense, high quality electrolyte, with some closed pores and the grain size is in micron-scale between 0.5-13 µ.

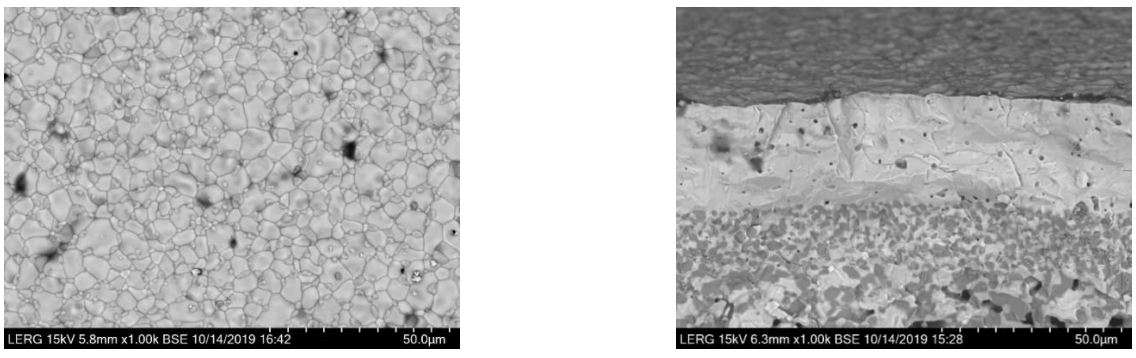

(a) (b)

Figure 6. SEM images of the surface (a) and fractured surface (b) of BCZYZ layer

4 Conclusions

BCZYZ suspensions with solid loadings in range of 8-23 vol.% exhibit a transition from shear-thinning to Newtonian behaviour in shear rate around 2 s^{-1} for low solid loadings and 10-20 s^{-1} for high solid loadings. While the difference in the apparent viscosity at low and high shear rates are negligible at low solid loadings up to 16 vol.%, it becomes significant at higher solid loadings. Therefore, the effect of coating parameters (such as withdrawal speed, diameter of coating vessel etc) on the electrolyte thickness cannot be negligible for the high solid loading slurries.

Zeta potential measurements indicates that 11 vol.% solid loading leads the isoelectric point and makes the suspension very unstable around that solid loading. The sedimentation results show that the stability of the suspension is very poor under 11 vol.% solid loading, and it becomes quite stable with the solid loading of 16 vol.% and above. The maximum solid loading has been predicted using Krieger-Dougherty equation and found as 25 vol.% at the high and medium shear rates and 24 vol.% at the low shear rates. However, as the viscosity increases above 16 vol.% solid loading, this solid loading has been identified as the max solid loading can be achieved without giving any compromise in coating thinness or quality.

A dip-coating slurry formulated with the maximum solid loading has been used to coat an electrolyte layer on the porous L025 NiO/BCZYZ tubular supports. SEM analysis indicates that 30µ thick, very dense electrolyte layer has successfully been achieved with some closed pores. The thickness of the electrolyte layer can be reduced by optimising dip-coating parameters for proton conducting solid oxide fuel cell and electrolyser applications.

Acknowledgement

Low Emissions Resources Global Ltd. (LERG) is a wholly owned subsidiary of Low Emissions Resources Corporation (LERC). This work did not receive any specific grant from funding agencies in the public, commercial, or not-for-profit sectors.

Conflict of interest

The authors declare that there is no conflict of interest.

Similarity rate (iThenticate): .13%

References

[1] A. Torabi, T.H. Etsell, P. Sarkar, Dip coating fabrication process for micro-tubular SOFCs. Solid State Ionic, 192, 372-375, 2011. https://doi.org/10.1016/j.ssi.2010.09.050

[2] B. Shri Prakash, S. Senthil Kumar and S.T. Aruna, Properties and development of Ni/YSZ as an anode material in solid oxide fuel cell: a review. Renewable and Sustainable Energy Reviews, 36, 149–179, 2014. https://doi.org/10.1016/j.rser.2014.04.043

[3] J.T.S Irvine and P. Connor, Solid oxide fuel cells: Facts and Figures. Springer London, 2013.

[4] C. Jia, M. Chen and M. Han, Performance and electrochemical analysis of solid oxide fuel cells based LSCF-YSZ nano-electrode, International Journal of Applied Ceramic Technology, 14 (5), 1006-1012, 2017. https://doi.org/10.1111/ijac.12748

[5] K.R. Lee, C.J. Tseng, S.C. Jang, J.C. Lin, K.W. Wang, J.K. Chang, T.C. Chen and S.W. Lee, Fabrication of anode-supported thin BCZY electrolyte protonic fuel cells using NiO sintering aid, International Journal of Hydrogen Energy 44, 23784-23792, 2019. https://doi.org/10.1016/j.ijhydene.2019.07.097

[6] Y. Meng, J. Gao, H. Huang, M. Zou, J. Duffy, J. Tong and K.S. Brinkman, A high-performance reversible protonic ceramic electrochemical cell based on a novel Sm-doped $BaCe_{0.7}Zr_{0.1}Y_{0.2}O_{3-\delta}$ electrolyte, Journal of Power Sources 439, 227093-227097, 2019. https://doi.org/10.1016/j.jpowsour.2019.227093

[7] A. Mat, M. Canavar, B. Timurkutluk and Y. Kaplan, Investigation of micro-tube solid oxide fuel cell fabrication using extrusion method, International Journal of Hydrogen Energy, 41, 10037-10043, 2016. https://doi.org/10.1016/j.ijhydene.2015.12.203

[8] C. Timurkutluk, K. Bilgil, A. Celen, S. Onbilgin, T. Altan and U. Aydin, Experimental investigation on the effect of anode functional layer on the performance of anode supported micro-tubular SOFCs, International Journal of Hydrogen Energy, https://doi.org/10.1016/j.ijhydene.2021.09.260

[9] S. Onbilgin, B. Timurkutluk, C. Timurkutluk and S. Celik, Comparison of electrolyte fabrication techniques on the performance of anode supported solid oxide fuel cells, International Journal of Hydrogen Energy, 45, 35162-35170, 2020. https://doi.org/10.1016/j.ijhydene.2020.01.097

[10] R.Z. Liu, S.R. Wang, B. Huang, C.H. Zhao, J.L. Li, Z.R. Wang, Z.Y. Wen and T.L. Wen, Dip-coating and co-sintering technologies for fabricating tubular solid oxide fuel cells, Journal of Solid State Electrochemistry, 13, 1905-1911, 2009. https://doi.org/10. 1007/s10008-008-0752-7

[11] L. Lei, Y. Bai, Y. Liu and J. Liu, An investigation on dip-coating techniques for fabricating anode-supported solid oxide fuel cells, International Journal of Applied Ceramic Technology, 12 (2), 351-357, 2015. https://doi.org/10.1111/ijac.12147

[12] C. Timurkutluk, B. Timurkutluk and Y. Kaplan, Experimental optimization of the fabrication parameters for anode-supported micro-tubular solid oxide fuel cells, International Journal of Hydrogen Energy 45, 23294-23309, 2020. https://doi.org/10.1016/j.ijhydene.2020.06.060

[13] R. De la Torre Garcia, Production of micro-tubular solid oxide fuel cells. PhD Thesis, University of Trento, Trento, Italy, 2011.

[14] Z. Hu, Y. Yang, Q. Chang, F. Liu, Y. Wang and J. Rao, Preparation of a high-performance ceramic membrane by a two-step coating method and one-step sintering, Applied Sciences, 9, 52-63, 2019. https://doi.org/10.3390/app9010052

[15] X. Li, H. Zhong, J. Zhang, Y. Duan, H. Bai and J. Li, D. Jiang, Dispersion and properties of zirconia suspensions for stereolithography, International Journal of Applied Ceramic Technology, 00, 1-9, 2019. https://doi.org/10.1111/ijac.13321

[16] A. De La Rosa, G. Ruiz, E. Castillo and R. Moreno, Calculation of dynamic viscosity in concentrated cementitious suspensions: Probabilistic approximation and Bayesian analysis, Materials (Basel), 14(8), 1971-1998, 2021. https://doi.org/10.3390/ma14081971

[17] A. Azzolini, V.M. Sglavo and J.A. Downs, Novel method for the identification of the maximum solid loading suitable for optimal extrusion of ceramic pastes, Journal of Advanced Ceramics, 3(1), 7-16, 2014. https://doi.org/10.1007/s40145-014-0088-y

[18] L.F.G. Setz, L. Koshimizu, S.R.H. Mello-Castanho and M.R. Morelli, Rheological analysis of ceramics suspensions with high solid loadings, Materials Science Forum, 727-728, 646-651, 2012. https://doi.org/10.4028/www.scientific.net/MSF.727-728.646

[19] P.K. Senapati, D. Panda and A. Parida, Predicting viscosity of limestone-water slurry, Journal of Minerals and Materials Characterization and Engineering, 8(3), 203-221, 2009. https://doi.org/10.4236/JMMCE.2009.83018

[20] B. PFG, Concentration effects in the rheology of cement pastes: Krieger-Dougherty revisited. Proceedings of 13th International Congress on the Chemistry of Cement, Madrid, Spain, 2011.